Inorg. Chem. **2006**, *45*, 710–716

$E_2(CN)_2$ (E = S, Se) and Related Compounds

Colin J. Burchell, Petr Kilian, Alexandra M. Z. Slawin, and J. Derek Woollins*

Department of Chemistry, University of St. Andrews, St. Andrews, Fife KY16 9ST, Scotland, U.K.

Karla Tersago, Christian Van Alsenoy, and Frank Blockhuys

Department of Chemistry, University of Antwerp, Universiteitsplein 1, B-2610 Wilrijk, Belgium

Received September 5, 2005

A synthetic, spectroscopic, and theoretical study of $E_x(CN)_2$ (E = S, Se; x = 1–3) is described. The X-ray structures of $Se_2(CN)_2$ and $Se_3(CN)_2$ have been determined. $Se_2(CN)_2$ crystallizes in a chiral space group with the CN groups approximately gauche.

Introduction

The pseudo-halogens are an interesting class of compounds that are rather understudied compared to simple halogen systems. There has recently been a report on $Te_x(CN)_2$,[1] and a new synthesis of $S_3(CN)_3$ has been developed.[2] As part of a broader study into $(SCN)_x$ and $(SeCN)_x$, we have reinvestigated $Se_x(CN)_2$ ($x = 1-3$), which was originally prepared by Birckenbach and Kellermann in 1925.[3] The X-ray crystal structures of $Se(CN)_2$[4a] and $Se(SeCN)_2$[4b] have both been reported, but the structure of $Se_2(CN)_2$ has remained elusive, in part because the compound readily disproportionates.[5] The sulfur analogues are also rather poorly characterized spectroscopically, though the X-ray structures of $S(CN)_2$ and $S(SCN)_2$ are known.[6]

Here we provide spectroscopic data on the homologous series $E_x(CN)_2$ (E = S, Se; $x = 1-3$) as well as X-ray structure determinations for $Se_2(CN)_2$ and $Se_3(CN)_2$. Furthermore, we have conducted quantum chemical calculations on the two homologous series, the results of which are compared to the experimental spectroscopic and structural data.

* To whom correspondence should be addressed. E-mail: jdw3@st-and.ac.uk.

(1) Klapotke, T. M.; Krumm, B.; Galvesz-Ruiz, J. C.; Noth, H.; Schwab, I. *Eur. J. Inorg. Chem.* **2004**, *24*, 4764.
(2) Kachanov, A.; Slabko, Yu.; Branova, O. V.; Shilova, E. V.; Kaminskii, V. A. *Tetrahedron Lett.* **2004**, *45*, 4461.
(3) (a) Birckenbach, L.; Kellermann, K. *Chem. Ber.* **1925**, *58*, 786. (b) Birckenbach, L.; Kellermann, K. *Chem. Ber.* **1925**, *58*, 2377.
(4) (a) Linke, K. H.; Lemmer, F. *Z. Anorg. Allg. Chem.* **1966**, *345*, 211. (b) Aksnes, O.; Foss, O. *Acta Chem. Scand.* **1954**, *8*, 1787.
(5) Aynsley, E. E.; Greenwood, N. N.; Sprague, A. *J. Chem. Soc.* **1964**, 704.
(6) (a) Feher, F.; Hirschfeld, D.; Linke, K. H. *Acta Crystallogr.* **1963**, *16*, 154. (b) Hazell, A. C. *Acta Crystallogr.* **1963**, *16*, 843. (c) Emerson, K. *Acta Crystallogr.* **1966**, *21*, 970.

Results and Discussion

Thiocyanogen [$S_2(CN)_2$, **1**] was synthesized by the reaction of silver thiocyanate with bromine in sulfur dioxide below −20 °C (eq 1). We have also carried out the reaction in

$$2Ag(SCN) + Br_2 \rightarrow 2AgBr + S_2(CN)_2 \qquad (1)$$

chloroform, dichloromethane, and diethyl ether, but sulfur dioxide was found to be the solvent that gave the cleanest reaction and was readily removed at low temperature. The mixture was filtered to remove precipitated silver bromide and the solvent removed in vacuo. The product was isolated in good yield as a colorless crystalline solid that was stable only when maintained at temperatures below −20 °C. In solution, **1** is slightly more stable and can be stored without significant change (assessed spectroscopically) at temperatures below 0 °C. On allowing **1** to warm slowly, the colorless crystals melt to give a yellow liquid before spontaneously polymerizing to give polythiocyanogen as an amorphous brick-red solid. **1** is readily soluble in chlorinated solvents such as chloroform and dichloromethane and nonhalogenated solvents such as tetrahydrofuran and diethyl ether. Because of thermal instability, no microanalytical or mass spectral data have been obtained. **1** exhibits a single $^{13}C\{^1H\}$ NMR ($CDCl_3$, −20 °C) resonance at $\delta(C) = 108.3$ ppm, which is comparable to the value recorded by Cataldo[7] (107.4 ppm in $CDCl_3$). **1** shows a single peak at $\delta(N) = 286.6$ ppm in the ^{14}N NMR ($CDCl_3$) spectrum (Table 1).

The IR spectrum (Table 2) shows a strong ν(C≡N) band at 2161 cm^{-1}, a ν(C−S) band at 669 cm^{-1}, a ν(S−S) band at 492 cm^{-1}, and two δ(S−C≡N) bands at 404 and 372

(7) Cataldo, F. *Polyhedron* **2000**, *19*, 681.

10.1021/ic0515103 CCC: $33.50
Published on Web 12/21/2005

Table 1. $^{13}C\{^1H\}$ NMR (67.9 MHz), ^{14}N NMR (21.7 MHz), and ^{77}Se NMR (67.9 MHz) Data

compound	δ(C) (ppm)[a]	δ(N) (ppm)	δ(Se) (ppm)
KSCN[b]	133.8	211.4	
1, $S_2(CN)_2$[c]	108.3 [114.5]	286.6 [354.0]	
2, $S(CN)_2$[d]	100.1 [105.0]	293.4 [338.4]	
KSeCN[b]	120.7	243.9	−342.3
4, $Se_2(CN)_2$[c]	96.0 [116.8]	298.5 [364.0]	0.45 [575.1]
5, $Se(CN)_2$[d]	91.5 [106.9]	299.8 [355.2]	0.29 [574.87]

[a] Values in square brackets are calculated (B3LYP/6-311+G*). [b] Recorded in D_2O at 25 °C. [c] Recorded in $CDCl_3$ at −20 °C. [d] Recorded in CD_2Cl_2 at −20 °C. **3** and **6** did not have sufficient solubility to record NMR data.

cm^{-1}. The Raman spectrum shows bands at 2158, 668, 494, and 397 cm^{-1} corresponding to ν(C≡N), ν(C−S), ν(S−S), and δ(S−C≡N), respectively. These observations are in accord with the literature IR and Raman data,[7,8] and our observed data are modeled well by the calculations. The single resonances in both the $^{13}C\{^1H\}$ and ^{14}N NMR spectra show that there is only one carbon and one nitrogen environment in the molecule. These observations and the ν(S−S) band present in the IR and Raman spectra concur with the proposed disulfide-bridged structure of **1**.

Sulfur dicyanide [$S(CN)_2$, **2**] and sulfur dithiocyanate [$S(SCN)_2$, **3**] were prepared for comparison by the reaction of sulfur dichloride in dichloromethane at 0 °C with silver cyanide (eq 2) and silver thiocyanate, respectively.

$$SCl_2 + 2AgCN \longrightarrow \text{N≡C–S–C≡N} + 2AgCl \qquad (2)$$

After filtration to remove precipitated AgCl, the solvent was removed in vacuo to give a colorless crystalline solid in both cases. **2** and **3** were both found to be stable when kept below 0 °C. Because of thermal instability, no microanalytical or mass spectral data have been obtained. **2** displays a single $^{13}C\{^1H\}$ NMR (CD_2Cl_2, −20 °C) resonance at δ(C) = 100.1 ppm and δ(N) = 293.4 ppm in the ^{14}N NMR (CD_2Cl_2, −20 °C) spectrum. No NMR data were obtained for **3** because of insufficient solubility. IR and Raman data for both species (Tables 3 and 4) are in agreement with published data[7] and are assigned by comparison with the calculated data. Note that for **3** two conformers were found in the gas phase, one with C_s symmetry and one with C_2 symmetry; the latter is a mere 3.22 kJ mol^{-1} more stable than the former. Both sets of vibrational data are presented in Table 4. The calculated bond lengths and angles for **2** and its selenium analogue, **5**, are given in Table 5.

The reaction of silver selenocyanate with iodine in liquid sulfur dioxide at −20 °C, after filtering to remove precipitated silver iodide, results in the formation of selenocyanogen [$Se_2(CN)_2$, **4**; eq 3) as a yellow crystalline solid in good yield (74%).

$$2Ag(SeCN) + I_2 \rightarrow 2AgI + Se_2(CN)_2 \qquad (3)$$

4 exhibits a single $^{13}C\{^1H\}$ NMR ($CDCl_3$, −20 °C) resonance at δ(C) = 96.0 ppm, a single ^{14}N NMR ($CDCl_3$, −20 °C) resonance at δ(N) = 298.5 ppm, and a single ^{77}Se NMR ($CDCl_3$, −20 °C) resonance at δ(Se) = 0.45 ppm, in agreement with the proposed diselenide-bridged structure. Cataldo had previously reported the $Se_2(CN)_2$ $^{13}C\{^1H\}$ NMR ($CDCl_3$) resonance at δ(C) = 89.92 ppm.[7] However, the sample was reported to be prepared at 13 °C before the solvent was distilled off under reduced pressure in a water bath. **4** is thermally unstable, and under these conditions, it is very likely that decomposition occurred to selenium dicyanide [$Se(CN)_2$, **5**] and selenium diselenocyanate [$Se(SeCN)_2$, **6**], as discussed below. The shift recorded by Cataldo is much closer to **5** [$^{13}C\{^1H\}$ NMR ($CDCl_3$): δ(C) = 91.5 ppm] rather than **4**.

The Raman spectrum of **4** contains (Table 2) a strong ν(C≡N) band at 2157 cm^{-1}, a medium ν(C−Se) band at 523 cm^{-1}, and a weak δ(Se−C≡N) band at 380 cm^{-1}, which agree with the previously published vibrational spectroscopic data.[5,7] No IR data were obtained because thermal instability prohibited the preparation of samples. Thermal instability also prevented us from recording mass spectra or microanalytical data. A single-crystal X-ray diffraction (XRD) study of **4** confirmed the diselenide-bridged structure (Figure 1 and Table 6). The Se−Se bond length is 2.356(1) Å, which is similar to the value in diselenium dihalides $(SeX)_2$ (X = Br, Cl),[7] which have Se−Se bonds of 2.241(1) and 2.232(1) Å, respectively. The C≡N bonds are typical for nitrile groups at 1.145(6) and 1.157(6) Å. In common with the structures of the related parent halides E_2X_2 (E = S, Se; X = Cl, Br),[9] the cyano groups are arranged in an approximately gauche relationship [C−Se−Se−C torsion angle 86.8(2)° compared to 83.9−87.4° in E_2X_2], reflecting the importance of the lone pairs in conformational control. As a consequence of this gauche arrangement, E_2X_2 molecules (including hydrogen peroxide) are chiral. To date, all previous structures have contained both enantiomers, but in the case of **4**, the compound spontaneously resolves and crystallizes in the space group $P2_{(1)}2_{(1)}2_{(1)}$. **4** is among the smallest species to have been crystallized as a single enantiomer. The packing diagram (Figure 2) clearly illustrates the importance of intermolecular interactions [Se(1)···N(1′) 2.876 Å, Se(1)···N(2″) 2.936 Å, Se(2)···N(1′) 3.199 Å, and Se(2)···N(2″) 3.157 Å]. We have no evidence that the compound is synthesized as one optical isomer and believe that this structure elegantly illustrates the ability of intermolecular interactions to control solid-state packing with the spontaneous crystallization of one isomer.

4 does not readily polymerize like the sulfur analogue **1**. Instead, when **4** is allowed to warm slowly, it disproportionates to give a mixture of **5** and **6** (eq 4).

$$2\ \text{N≡C–Se–Se–C≡N} \longrightarrow \text{N≡C–Se–C≡N} + \text{N≡C–Se–Se–Se–C≡N} \qquad (4)$$

(8) (a) Bacon, R. G. R.; Irwin, R. S. *J. Chem. Soc.* **1958**, 778. (b) Nelson, M. J.; Pullin, A. D. E. *J. Chem. Soc.* **1960**, 604. (c) Vanderzee, C. E.; Quist, A. S. *Inorg. Chem.* **1966**, *5*, 1238.

(9) Kniep, R.; Korte, L.; Mootz, D. *Z. Naturforsch.* **1983**, *38b*, 1.

Table 2. Calculated Vibrational Frequencies (ν_{calcd}) and IR Intensities (I_{calcd}) and Experimental IR (CH_2Cl_2, $\nu_{exptl,IR}$) and Raman ($\nu_{exptl,R}$) Vibrational Frequencies of $S_2(CN)_2$ and $Se_2(CN)_2$[a]

	$S_2(CN)_2$ (**1**)					$Se_2(CN)_2$ (**4**)		
	ν_{calcd}	I_{calcd}	$\nu_{exptl,IR}$	$\nu_{exptl,R}$[b]	assignment	ν_{calcd}	$\nu_{exptl,R}$[c]	assignment
a	2253	2		2158vs	ν_s(CN)	2250	2144s	ν_s(CN)
	675	3	669s	668vw	ν_s(CS)	522	513m	ν_s(CSe)
	453	1	492m	494w	ν(SS) + β_s(SSC)	368	380w	δ_s(SeCN) + β_s(SeCN)
	402	1	404w	397m	δ_s(SCN)	364		δ_s(SeCN) + β_s(SeCN)
	362	0			ν(SS) + β_s(SCN)	257	268vs	ν(SeSe)
	134	0			β_s(SSC) + β_s(SCN)	98		β_s(SeSeC)
	54	4			τ(SS)	47		τ(SeSe)
b	2258	3	2161vs		ν_{as}(CN)	2254	2157s	ν_{as}(CN)
	682	5			ν_{as}(CS)	525	523m	ν_{as}(CSe)
	423	1			β_{as}(SCN) + β_{as}(SSC)	371		β_{as}(SeCN)
	371	2	372w		δ_{as}(SCN)	339		δ_{as}(SeCN)
	149	8			β_{as}(SSC) + β_{as}(SCN)	106		β_{as}(SeSeC)

[a] Wavenumbers in cm^{-1} and intensities in km mol^{-1}. The assignments are based on the PED values and C_2 symmetry: ν, stretching mode; β, bending mode; δ, out-of-plane mode; τ, torsional mode; vs, very strong; s, strong; m, medium; w, weak; vw, very weak. [b] CH_2Cl_2. [c] Solid.

Table 3. Calculated Vibrational Frequencies (ν_{calcd}) and IR Intensities (I_{calcd}) and Experimental IR (KBr, $\nu_{exptl,IR}$) and Raman (solid, $\nu_{exptl,R}$) Vibrational Frequencies of $S(CN)_2$ and $Se(CN)_2$[a]

	$S(CN)_2$ (**2**)					$Se(CN)_2$ (**5**)				
	ν_{calcd}	I_{calcd}	$\nu_{exptl,IR}$	$\nu_{exptl,R}$	assignment	ν_{calcd}	I_{calcd}	$\nu_{exptl,IR}$	$\nu_{exptl,R}$	assignment
a_1	2292	2		2196vs	ν_s(CN)	2282	0		2188vs	ν_s(CN)
	682	8	697m	693m	ν_s(CS)	540	8		512vs	ν_s(CSe)
	498	2		509m	β(CSC)	445	1		454m	β(CSeC)
	123	8			β(CSC) + β_s(SCN)	106	7			β(CSeC) + β_s(SeCN)
a_2	366	0		389m	δ_s(SCN)	344	0	338w	343w	δ_s(SeCN)
b_1	352	3	379m		δ_{as}(SCN)	324	2	305m	309w	δ_{as}(SeCN)
b_2	2276	11	2184vs		ν_{as}(CN)	2269	3	2179vs		ν_{as}(CN)
	681	2	670m	675m	ν_{as}(CS)	524	6	509vs		ν_{as}(CSe)
	320	1			β_{as}(SCN)	293	1	279w		β_{as}(SeCN)

[a] Wavenumbers in cm^{-1} and intensities in km mol^{-1}. The assignments are based on the PED values and C_{2v} symmetry: ν, stretching mode; β, bending mode; δ, out-of-plane mode; vs, very strong; m, medium; w, weak.

Table 4. Calculated Vibrational Frequencies (ν_{calcd}) and IR Intensities (I_{calcd}) and Experimental IR (KBr, $\nu_{exptl,IR}$) and Raman (glass capillary, $\nu_{exptl,R}$) Vibrational Frequencies of $S(SCN)_2$

	C_2						C_s		
	ν_{calcd}	I_{calcd}	assignment	$\nu_{exptl,IR}$	$\nu_{exptl,R}$		ν_{calcd}	I_{calcd}	assignment
a	2257	0	ν_s(CN)		2156vs	*a*′	2259	4	ν_s(CN)
	673	0	ν_s(CS)		672w		674	7	ν_s(CS)
	454	0	ν_s(SS)	489m	492m		461	2	ν_s(SS) + β_s(SSC)
	395	1	β_s(SCN) + β_s(SSC)				395	1	ν_s(SS) + β_s(SCN)
	386	2	δ_s(SCN)				381	2	δ_s(SCN)
	191	1	β(SSS)		202m		187	2	β(SSS) + β_s(SCN)
	111	2	β_s(SCN) + β_s(SSC)				168	3	β(SSS) + β_s(SSC)
	41	5	τ_s(SS)				53		τ_s(SS)
b	2256	16	ν_{as}(CN)	2153vs		*a*″	2258	4	ν_{as}(CN)
	672	6	ν_{as}(CS)	668m			673	0	ν_{as}(CS)
	432	5	β_{as}(SCN) + β_{as}(SSC)	454m	458m		424	4	ν_{as}(SS) + β_{as}(SCN) + β_{as}(SSC)
	387	5	δ_{as}(SCN)	400m			385	0	δ_{as}(SCN)
	378	19	ν_{as}(SS)				374	19	ν_{as}(SS)
	177	4	β_{as}(SSC) + β_{as}(SCN)				122	6	β_{as}(SSC) + β_{as}(SCN)
	61	6	τ_{as}(SS)				48	1	τ_{as}(SS)

[a] Wavenumbers in cm^{-1} and intensities in km.mol^{-1}. The assignments are based on the PED values and C_2 or C_s symmetry. ν stretching mode; β bending mode; δ out-of-plane mode; τ torsional mode; vs very strong; s strong; m medium; w weak.

No visible change was noted because **5** is colorless and **6** is also a yellow crystalline solid; however, the disproportionation was followed spectroscopically. When **4** began to disproportionate, a new peak was noted in the $^{13}C\{^1H\}$ NMR ($CDCl_3$) spectrum at 90.6 ppm corresponding to **5**. No peak was observed for **6** because of its poor solubility. Disproportionation was also observed in the Raman spectrum by the emergence of two new cyanide stretches at 2188 and 2144 cm^{-1} corresponding to **5** and **6**, respectively.

Both **5** and **6** have been previously reported in the literature[2,7,10] and studied by single-crystal XRD.[3,4] However, it was necessary to resynthesize both to obtain accurate spectral data for comparison with **4**. **5** was prepared by the reaction of 2 equiv of silver cyanide with selenium dichloride (prepared in situ by reacting selenium powder with sulfuryl chloride) in tetrahydrofuran. Removal of the solvent under reduced pressure followed by extraction of the residue with dichloromethane furnished, after filtration through Celite (to remove solid AgCl) and evaporation of the filtrate to dryness, the product was a white powdery solid in 66% yield.

(10) (a) Kaufmann, H. P.; Kogler, F. *Chem. Ber.* **1926**, *59*, 178. (b) Cauquis, G.; Pierre, G. *Bull. Soc. Chim. Fr.* **1972**, *N3*, 1225.

Table 5. Geometrical Data Comparing the Solid-State (XRD) and Calculated Gas-Phase (B3LYP/6-311+G*, r_e) Structures of $S(CN)_2$ (E = S) and $Se(CN)_2$ (E = Se)[a]

	$S(CN)_2$ (**2**)				$Se(CN)_2$ (**5**)		
	XRD[b]		B3LYP	BO	XRD[c]	B3LYP	BO
E(1)−C(1)	1.74(2)	1.72(2)	1.71	1.42	1.86(10)	1.86	1.27
C(1)−N(1)	1.12(2)	1.13(2)	1.16	2.91	1.42(15)	1.16	2.92
C(1′)−E(1)−C(1)	95.6(8)		99.6		119(6)	97	
E(1)−C(1)−N(1)	177(1)	176(2)	175		177(6)	175	

[a] Bond lengths in Å and angles in deg. Calculated Hirshfeld bond orders (BO) are given for the corresponding bonds. [b] Two symmetry-independent molecules in the asymmetric unit [5]. [c] Reference 6.

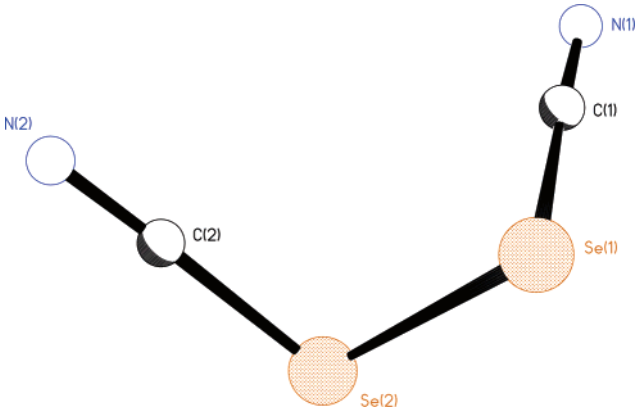

Figure 1. X-ray crystal structure of **4**.

Table 6. Geometrical Data Comparing the Solid-State (XRD) and Calculated Gas-Phase (B3LYP/6-311+G*, r_e) Structures of $S_2(CN)_2$ and $Se_2(CN)_2$[a]

		XRD	B3LYP	BO
1, $S_2(CN)_2$	S(1)−S(2)		2.1423	0.91
	S(1)−C(1)		1.6982	1.50
	S(2)−C(2)		1.6982	1.50
	C(1)−N(1)		1.1587	2.90
	C(2)−N(2)		1.1587	2.90
	S(1)−S(2)−C(2)		101.33	
	S(2)−S(1)−C(1)		101.33	
	S(1)−C(1)-N(1)		175.51	
	S(2)−C(2)−N(2)		175.51	
	C(1)−S(1)−S(2)−C(2)		88.96	
4, $Se_2(CN)_2$	Se(1)−Se(2)	2.3558(7)	2.3854	0.89
	Se(1)−C(1)	1.867(5)	1.852	1.32
	Se(2)−C(2)	1.855(5)	1.852	1.32
	C(1)−N(1)	1.145(6)	1.159	2.91
	C(2)−N(2)	1.156(7)	1.159	2.91
	Se(2)−Se(1)−C(1)	95.33(12)	99.59	
	Se(1)−Se(2)−C(2)	95.99(13)	99.59	
	Se(1)−C(1)−N(1)	176.2(4)	183.6	
	Se(2)−C(2)−N(2)	178.3(4)	183.6	
	C(1)−Se(1)−Se(2)−C(2)	−86.8(2)	91.0	

[a] Bond lengths in Å and angles in deg. Calculated Hirshfeld bond orders (BOs) are given for the corresponding bonds. The XRD data for $S_2(CN)_2$ comes from ref 6.

Although no decomposition of **5** was noted, the sample was stored under a nitrogen atmosphere at 0 °C as a precaution. Microanalysis was within acceptable limits and positive ion electrospray ionization mass spectroscopy (EI-MS) showed the expected M^+ and other fragments. **5** exhibits a single $^{13}C\{^1H\}$ NMR (CD_2Cl_2, −20 °C) resonance at $\delta(C) = 91.5$ ppm, a single ^{14}N NMR (CD_2Cl_2) resonance at $\delta(N) = 299.8$ ppm, and a single ^{77}Se NMR (CD_2Cl_2) resonance at $\delta(Se) = 0.29$ ppm. The IR and Raman spectra displayed the anticipated bands (Table 3) for the C≡N, C−Se, and Se−C≡N functionalities.

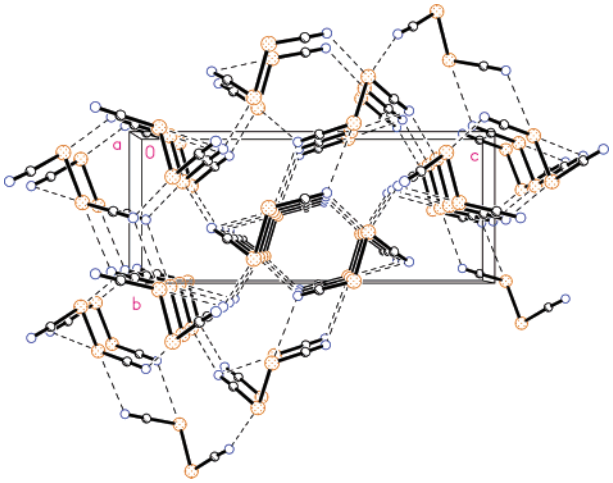

Figure 2. Packing in the solid-state structure of **4**.

6 was prepared in a fashion analogous to that of **5** by reacting 2 equiv of silver selenocyanate with selenium dichloride in tetrahydrofuran. After a workup similar to that used above, the product was isolated as a bright yellow crystalline solid in a 71% yield. When left to stand at room temperature, it was noted that some decomposition occurred, producing a red solid, which is probably selenium. As a result, **6** was stored under a nitrogen atmosphere at 0 °C and no further decomposition was observed. Microanalysis and positive ion EI-MS showed the expected results. **6** was found to have poor solubility in organic solvents, and therefore no NMR data were recorded. The IR spectrum (Table 7) shows a strong ν(C≡N) band at 2141 cm^{-1}, a medium ν(C−Se) band at 511 cm^{-1}, and a weak δ(Se−C≡N) band at 362 cm^{-1}. In addition, the Raman spectrum also showed the anticipated bands (Table 7). Note that for **6** the calculations found two conformers in the gas phase, one with C_s symmetry and one with C_2 symmetry; the latter is a mere 3.68 kJ mol^{-1} more stable than the former. Both sets of vibrational data have been presented in Table 7. The crystal structure of **6** was obtained (Table 8 and Figure 3).

The geometrical results of the calculations at the DFT/B3LYP/6-311+G* level are compared to the available experimental data for $E(CN)_2$ in Table 6, for $E_2(CN)_2$ in Table 5, and for $E_3(CN)_2$ in Table 8; calculated Hirshfeld bond orders are also given. According to the calculations, the optimized $E(CN)_2$ (E = S, Se) geometries have C_{2v} symmetry. The calculated parameters (Table 6) show the same trend as the experimental values. Substituting sulfur by selenium gives longer and thus weaker bonds, as can be seen from the bond order values of the EC bonds, which are 1.42 vs 1.27 for SC and SeC, respectively. The fact that these values are considerable larger than 1 can be explained by the contribution of the $-S^+=C=N^-$ resonance form to the overall structure. Whether E is sulfur or selenium has virtually no effect on the nature of the CN triple bonds because they are of the same strength (2.91 vs 2.92) in both compounds.

Table 7. Calculated Vibrational Frequencies (ν_{calcd}) and IR intensities (I_{calcd}) and Experimental IR (KBr, $\nu_{exptl,IR}$) and Raman (Solid, $\nu_{exptl,R}$) Vibrational Frequencies of $Se(SeCN)_2$ (**6**)[a]

	C_2						C_s		
	ν_{calcd}	I_{calcd}	assignment	$\nu_{exptl,IR}$	$\nu_{exptl,R}$		ν_{calcd}	I_{calcd}	assignment
a	2251	0	ν_s(CN)		2144vs	*a′*	2253	1	ν_s(CN)
	520	1	ν_s(CSe)		509m		523	11	ν_s(CSe)
	373	0	β_s(SeCN)		383w		374	0	β_s(SeCN)
	353	1	δ_s(SCN)		360w		350	1	δ_s(SCN)
	262	0	ν_s(SeSe)	262w	270s		261	0	ν_s(SeSe)
	108	1	β(SeSeSe)				117	3	β_s(SeSeC)
	80	2	β(SeSeSe) + β_s(SeSeC)				94	0	β(SeSeSe)
	34	4	τ_s(SeSe)				43	1	τ_s(SeSe)
b	2251	9	ν_{as}(CN)	2141vs		*a″*	2252	2	ν_{as}(CN)
	519	12	ν_{as}(CSe)	511m			522	1	ν_{as}(CSe)
	374	1	β_{as}(SeCN)	362w			369	0	β_{as}(SeCN)
	351	0	δ_{as}(SCN)				351	1	δ_{as}(SCN)
	244	9	ν_{as}(SeSe)	247w			245	8	ν_{as}(SeSe)
	117	4	β_{as}(SeSeC)				93	6	β_{as}(SeSeC)
	42	5	τ_{as}(SeSe)				37	1	τ_{as}(SeSe)

[a] Wavenumbers in cm^{-1} and intensities in km mol^{-1}. The assignments are based on the PED values and C_2 or C_s symmetry: ν, stretching mode; β, bending mode; δ, out-of-plane mode; τ, torsional mode; vs, very strong; s, strong; m, medium; w, weak.

Table 8. Geometrical Data Comparing the Solid-State (XRD) and Calculated Gas-Phase (B3LYP/6-311+G*, r_e) Structures of $Se(SeCN)_2$ (**6**) and the Calculated Structure for $S(SCN)_2$ (**3**)[a]

Compound **6**

	C_s			C_2	
	XRD	B3LYP	BO	B3LYP	BO
Se(1)−Se(2)	2.3390(7)	2.3755	0.95	2.3759	0.95
Se(1)−C(1)	1.860(4)	1.853	1.32	1.854	1.32
C(1)−N(1)	1.145(5)	1.159	2.91	1.159	2.92
Se(2)−Se(1)−C(1)	96.60(9)	100.77		99.99	
Se(1)−Se(2)−Se(1′)	102.72(2)	106.02		105.79	
Se(1)−C(1)−N(1)	177.7(3)	183.9		182.7	
C(1)−Se(1)−Se(2)−Se(1′)	86.32(10)	−86.00		93.33	

Compound **3**

	C_s		C_2	
	B3LYP	BO	B3LYP	BO
S(1)−S(2)	2.1201	1.02	2.1209	1.01
S(1)−C(1)	1.7020	1.49	1.7020	1.49
C(1)−N(1)	1.1585	2.90	1.1586	2.91
S(1)−S(2)−S(1′)	107.66		107.61	
C(1)−S(1)−S(2)	102.70		102.02	
S(1)−C(1)−N(1)	175.43		176.38	
C(1)−S(1)−S(2)−S(1′)	92.64		−84.55	
C(1′)-S(1′)−S(2)−S(1)	−92.64		−84.55	
N(1)−C(1)-S(1)−S(2)	172.46		177.10	
N(1′)−C(1′)−S(1′)−S(2)	−172.46		177.10	

[a] Bond lengths in Å and angles in deg. Calculated Hirshfeld bond orders (BOs) are given for the corresponding bonds.

In the gas phase, $S_2(CN)_2$ and $Se_2(CN)_2$ have C_2 symmetry, which leads to a number of more pronounced geometrical differences with the experimental structure, of which the symmetry is C_{2v} (Table 5). A closer look at the bond orders again indicates that the replacement of sulfur by selenium leads to bonds that are longer and weaker: the values for SS and SeSe are 0.91 and 0.89, respectively, and for SC and SeC, the bond orders are 1.50 and 1.32, respectively. Equally, the effects of the replacement are limited to these bonds because the CN triple bonds are of the same strength (2.90 vs 2.91) in both compounds.

As mentioned above, for $S_3(CN)_2$ and $Se_3(CN)_2$, two energy minima were found: one with C_s symmetry and the two CN groups at the same side of the E_3 plane and one with C_2 symmetry and the two CN groups at different sides. The conformers with C_2 symmetry are stabilized over the C_s conformers by 3.22 and 3.68 kJ mol^{-1} for the sulfur and selenium analogues, respectively. The substitution of sulfur by selenium (Table 8) has the same effects on the geometry as those described above. Comparing the calculated C_s and C_2 geometries reveals that the effect of the symmetry on the bond strength is negligible because the differences in bond lengths are very small. It is interesting to note that the EC and CN distances remain fairly constant throughout the $E_x(CN)_2$ series and that this is true for both sulfur and selenium: thus, the bonding in these peripheral bonds is quite insensitive to the number of chalcogen atoms that connects them.

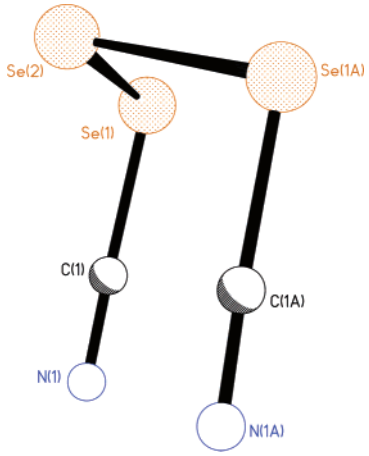

Figure 3. X-ray crystal structure of **6**.

The X-ray structure of **6** reveals (Table 8 and Figure 3) that the CN groups are eclipsed. The central Se−Se−Se angle at 102.72(2)° is slightly smaller than that derived from the calculations. The Se−Se bond length [2.390(7) Å] is marginally longer than that in $Se_2(CN)_2$ [2.3558(7) Å].

The pseudo-halogens $E_x(CN)_2$, which we have fully characterized here, are being increasingly utilized as chalcogen transfer agents for the synthesis of new organic compounds.[2] Furthermore, the spontaneous polymerization of $S_2(CN)_x$ leads to the poorly characterized $(SCN)_x$. We are

currently examining the spectroscopic data for this polymer in comparison with the data reported here and shall report on this in due course.

Experimental Section

Sulfur dioxide (BOC) was used as received. Chlorine (BOC) was dried by passing the gas over phosphorus pentoxide. Bromine, iodine, potassium thiocyanate, potassium selenocyanate, selenium, silver cyanide, and sulfuryl chloride (all Aldrich) were used as received. Sulfur dichloride was purified by distillation over a small amount of phosphorus trichloride. Silver thiocyanate and silver selenocyanate was prepared by mixing equimolar quantities of potassium thiocyanate or potassium selenocyanate, respectively, with silver nitrate (all Aldrich) in water.

Solution NMR spectra were recorded on JEOL DELTA 270 or Bruker AM300 instruments. $^{13}C\{^1H\}$ NMR (67.9 MHz), ^{14}N NMR (21.7 MHz), and ^{77}Se NMR (67.9 MHz) are referred to tetramethylsilane (TMS), $NH_3(l)$, and Me_2Se, respectively

$S_2(CN)_2$ (1). Silver thiocyanate (3.319 g, 0.02 mol) was suspended in sulfur dioxide (20 cm^3) with vigorous stirring, and bromine (1.598 g, 0.01 mol) was added dropwise. The mixture was stirred for 2 h below −20 °C. The loss of the red-brown color afforded by bromine indicated that the reaction was complete. The mixture was filtered to remove precipitated silver bromide, leaving the colorless solution of **1**. The sulfur dioxide was removed in vacuo below −20 °C to give **1** as a colorless crystalline solid. Yield: 0.801 g (69%). $^{13}C\{^1H\}$ NMR ($CDCl_3$, −20 °C): δ(C) = 108.3 ppm (S−C≡N, singlet). ^{14}N NMR ($CDCl_3$, −20°C): δ = 286.6 ppm (C≡N, singlet). IR (CH_2Cl_2): 2161vs, 1612w, 1098w, 669s, 492m, 404w, 372w cm^{-1}. Raman (CH_2Cl_2 glass capillary): 2160vs, 668w, 494s, 399m, 176m cm^{-1}.

$S(CN)_2$ (2). Dichloromethane (40 cm^3) was added to sulfur dichloride (0.697 g, 6.769 mmol) and the resultant solution cooled to 0 °C. Silver cyanide (1.813 g, 13.538 mmol) was then added, and the mixture was stirred for approximately 1 h. The reaction was observed to be complete when the red-brown color of sulfur dichloride had dissipated. The mixture was filtered to remove silver chloride followed by removal of solvent under reduced pressure below 0 °C to isolate the product as a white solid. Yield: 0.384 g (67%). $^{13}C\{^1H\}$ NMR (CD_2Cl_2, −20 °C): δ(C) = 100.1 ppm (S−C≡N, singlet). ^{14}N NMR (CD_2Cl_2, −20°C): δ = 294 ppm (C≡N, singlet). IR (KBr): 2184vs, 697m, 670m, 376m, 278w, 252w cm^{-1}. Raman (glass capillary): 2196vs, 693w, 675w, 509w, 389w cm^{-1}.

$S(SCN)_2$ (3). 3 was prepared in the same fashion as **2** using sulfur dichloride (0.908 g, 8.818 mmol) and silver thiocyanate (2.927 g, 17.636 mmol). The mixture was filtered to remove silver chloride followed by removal of solvent under reduced pressure below 0 °C to isolate the product as a white solid. Yield: 0.771 g (59%). IR (KBr): 2153vs, 668m, 489m, 454m, 400m, 280w, 253w, 230w cm^{-1}. Raman (glass capillary): 2156vs, 672w, 492m, 458w, 433m, 214m, 202m cm^{-1}.

$Se_2(CN)_2$ (4). 4 was prepared in the same fashion as **1** using silver selenocyanate (2.028 g, 9.526 mmol) and iodine (1.209 g, 4.763 mmol). The mixture was stirred for 2 h below −20 °C. The mixture was filtered to remove precipitated silver iodide, leaving the yellow solution of **4**. The sulfur dioxide was removed in vacuo below −20 °C to give **4** as a yellow crystalline solid. Yield: 0.742 g (74%). $^{13}C\{^1H\}$ NMR ($CDCl_3$, −20 °C): δ(C) = 96.0 ppm (Se−C≡N, singlet). ^{14}N NMR ($CDCl_3$, −20 °C): δ = 298.5 ppm (C≡N, singlet). ^{77}Se NMR ($CDCl_3$, −20 °C): δ = 0.45 ppm (Se−C≡N, singlet). Raman (glass capillary): 2157vs, 523m, 380w, 268s cm^{-1}.

Table 9. Details of the X-ray Data Collections and Refinements for **4** and **6**[a]

compound	**4**	**6**
empirical formula	$C_2N_2Se_2$	$C_2N_2Se_3$
crystal dimens/mm	0.18 × 0.05 × 0.05	0.10 × 0.10 × 0.02
cryst syst	orthorhombic	orthorhombic
space group	$P2_{(1)}2_{(1)}2_{(1)}$	*Pnma*
a/Å	5.04488(11)	10.054(2)
b/Å	6.4597(14)	13.332(3)
c/Å	15.589(3)	4.4540(10)
α/deg	90	90
β/deg	90	90
γ/deg	90	90
U/Å^3	508.01(19)	597.0(2)
Z	4	4
M	209.955	288.915
D_c/(g cm^{-3})	2.745	3.215
μ/mm^{-1}	14.395	18.354
measd reflns	2426	2043
independent reflns (R_{int})	708(0.0568)	392(0.0960)
final R1, wR2 [$I > 2\sigma(I)$]	0.0191, 0.0377	0.0218, 0.0494

[a] 4 = cbdw20; 6 = cbdw04.

$Se(CN)_2$ (5). Sulfuryl chloride (0.417 g, 3.090 mmol) was added to selenium powder (0.244 g, 3.090 mmol), and the mixture was stirred for 10 min. Then tetrahydrofuran (5 cm^3) was added, and the solution was stirred for 1 h to give a clear brown solution of selenium dichloride. Silver cyanide (0.827 g, 6.180 mmol) was added with tetrahydrofuran (20 cm^3), and the solution was stirred for 1 h. The solvent was then removed in vacuo, and dichloromethane (30 cm^3) was added. The solution was filtered through a Celite pad and washed with dichloromethane (20 cm^3), and the solvent was removed in vacuo to yield the product as a white solid. Yield: 0.268 g (66%). Anal. Found (calcd for $Se(CN)_2$): C, 18.91 (18.33); N, 21.26 (21.39). $^{13}C\{^1H\}$ NMR (CD_2Cl_2, −20 °C): δ(C) = 91.5 ppm (Se−C≡N, singlet). ^{14}N NMR (CD_2Cl_2, −20 °C): δ = 299.8 ppm (C≡N, singlet). ^{77}Se NMR (CD_2Cl_2, −20 °C): δ = 0.29 ppm (Se−C≡N, singlet). EI^+ MS: *m*/*z* 132 $[M]^+$, 106 $[M - CN]^+$. IR (KBr): 2926vw, 2179vs, 1261w, 1096w, 1024w, 802w, 509vs, 338m, 305m, 279w, 270w, 250w, 244w cm^{-1}. Raman (glass capillary): 2188vs, 512s, 454w, 343w, 309w, 178w cm^{-1}.

$Se(SeCN)_2$ (6). 6 was prepared in the same fashion as **5** using sulfuryl chloride (0.295 g, 2.186 mmol), selenium powder (0.173 g, 2.186 mmol), and silver selenocyanate (0.930 g, 4.371 mmol). The solvent was then removed in vacuo, and dichloromethane (30 cm^3) was added. The solution was filtered through a Celite pad and washed with dichloromethane (20 cm^3), and the solvent was removed in vacuo to yield the product as a yellow crystalline solid. Yield: 0.446 g (71%). Anal. Found (calcd for $Se(SeCN)_2$): C, 8.41 (8.31); N, 9.58 (9.70). EI^+ MS: *m*/*z* 292 $[M]^+$, 212 $[M - Se]^+$, 132 $[M - 2Se]^+$. IR (KBr): 2929vw, 2141vs, 511m, 362w, 280w, 262w, 247w cm^{-1}. Raman (glass capillary): 2144vs, 1491w, 509w, 383w, 360w, 270s cm^{-1}.

X-ray Crystallography. Table 9 lists details of data collections and refinements. Intensities were corrected for Lorentz polarization and for absorption. Data were collected at 125 K using a Bruker SMART system.The structures were solved by the heavy-atom method or by direct methods. The positions of the hydrogen atoms were idealized. Refinements were by full-matrix least squares based on F^2 using *SHELXTL*.[11]

Computational Details. Theoretical calculations were performed using *Gaussian03*[12] applying standard gradient techniques at the DFT/B3LYP level of theory using the 6-311+G* basis set on all atoms; this basis set was used because it is implemented in the

(11) Sheldrick, G. M. *SHELXTL*; Bruker AXS: Madison, WI, 1999.

program. All subsequent calculations of molecular properties were performed at the optimized B3LYP/6-311+G* geometries. Force-field calculations were used to ascertain whether the resulting structures were energy minima, and these calculations yielded the frequencies used in the vibrational analyses. No attempts were made to scale the force field. The Cartesian force field was transformed into one described in a set of pseudosymmetry coordinates[13,14] to construct the potential energy distribution (PED), which was subsequently used to derive approximate descriptions of the normal modes. Chemical shielding factors were calculated at all atomic positions at the DFT/B3LYP/6-311+G* level of theory using the GIAO method implemented in *Gaussian03*. The chemical shifts of the selenium atoms were obtained by subtracting their chemical shielding values from the one calculated for dimethylselenide, which is 1623.1500 ppm at the B3LYP/6-311+G* level of theory, based on the corresponding geometry (C_{2v} symmetry, anti,anti conformer). The chemical shifts for the carbon atoms were obtained by subtracting their chemical shielding values from the one calculated for TMS, which is 184.0193 ppm at the B3LYP/6-311+G* level of theory, based on the corresponding geometry. The chemical shifts for the nitrogen atoms were obtained by subtracting their chemical shielding values from the one calculated for ammonia (NH_3), which is 258.6697 ppm at the B3LYP/6-311+G* level of theory, based on the corresponding geometry. Bond orders were calculated according to the Hirshfeld scheme.[15]

Supporting Information Available: Crystallographic data for **4** and **6** in CIF format. This material is available free of charge via the Internet at http://pubs.acs.org.

IC0515103

(12) Frisch, M. J.; Trucks, G. W.; Schlegel, H. B.; Scuseria, G. E.; Robb, M. A.; Cheeseman, J. R.; Montgomery, J. A., Jr.; Vreven, T.; Kudin, K. N.; Burant, J. C.; Millam, J. M.; Iyengar, S. S.; Tomasi, J.; Barone, V.; Mennucci, B.; Cossi, M.; Scalmani, G.; Rega, N.; Petersson, G. A.; Nakatsuji, H.; Hada, M.; Ehara, M.; Toyota, K.; Fukuda, R.; Hasegawa, J.; Ishida, M.; Nakajima, T.; Honda, Y.; Kitao, O.; Nakai, H.; Klene, M.; Li, X.; Knox, J. E.; Hratchian, H. P.; Cross, J. B.; Bakken, V.; Adamo, C.; Jaramillo, J.; Gomperts, R.; Stratmann, R. E.; Yazyev, O.; Austin, A. J.; Cammi, R.; Pomelli, C.; Ochterski, J. W.; Ayala, P. Y.; Morokuma, K.; Voth, G. A.; Salvador, P.; Dannenberg, J. J.; Zakrzewski, V. G.; Dapprich, S.; Daniels, A. D.; Strain, M. C.; Farkas, O.; Malick, D. K.; Rabuck, A. D.; Raghavachari, K.; Foresman, J. B.; Ortiz, J. V.; Cui, Q.; Baboul, A. G.; Clifford, S.; Cioslowski, J.; Stefanov, B. B.; Liu, G.; Liashenko, A.; Piskorz, P.; Komaromi, I.; Martin, R. L.; Fox, D. J.; Keith, T.; Al-Laham, M. A.; Peng, C. Y.; Nanayakkara, A.; Challacombe, M.; Gill, P. M. W.; Johnson, B.; Chen, W.; Wong, M. W.; Gonzalez, C.; Pople, J. A. *Gaussian 03*, revision B.05; Gaussian, Inc.: Wallingford, CT, 2004.

(13) Pulay, P.; Fogarasi, G.; Pang, F.; Boggs, J. E. *J. Am. Chem. Soc.* **1979**, *101*, 2550−2560.

(14) Fogarasi, G.; Zhou, X. F.; Taylor, P. W.; Pulay, P. *J. Am. Chem. Soc.* **1992**, *114*, 8191−8201.

(15) Oláh, J.; Blockhuys, F.; Veszprémi, T.; Van Alsenoy, C., unpublished results.